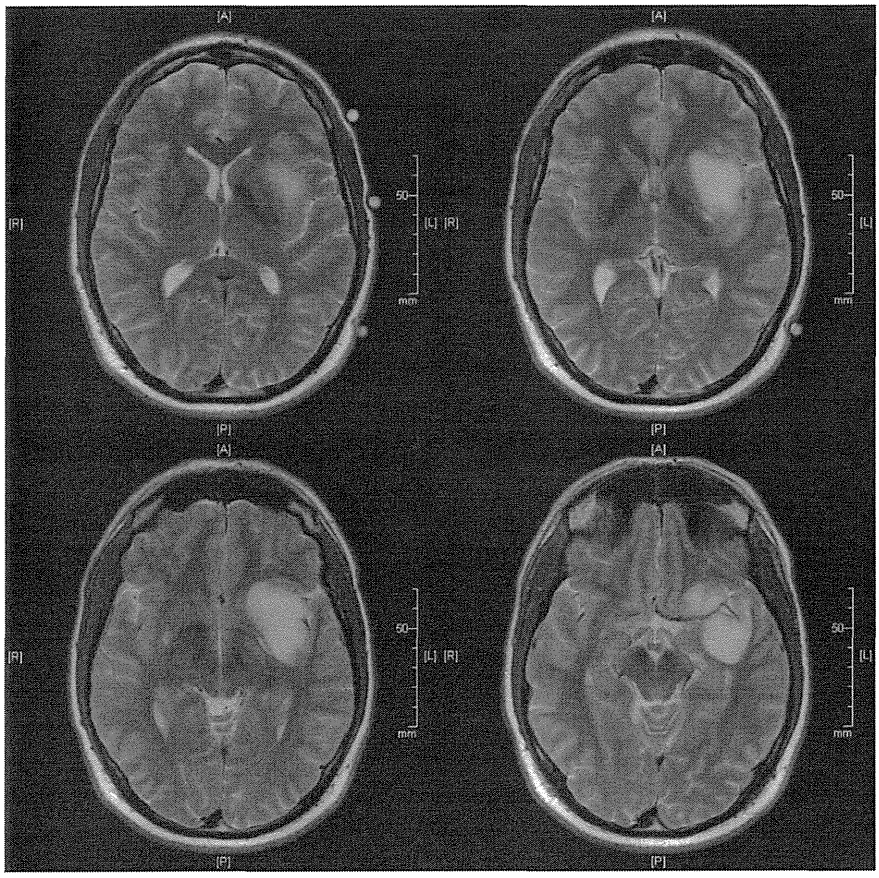

Fig. 1. Preoperative transaxial T1-weighted MR images showing a left frontotemporal low-grade astrocytoma, which involved the insula, temporal stem, and orbitofrontal cortex. A: anterior, P: posterior, R: right, L: left.

Intraoperative electrical stimulation inhibits the function of a restricted region of the brain [5], which makes it possible to observe real-time responses when the region has been functionally inhibited by the stimulation. There have been three reports on the effects of intraoperative stimulation in the dominant UF, each reporting a different reaction: semantic paraphasia [6], phonetic paraphasia [2], and no language disturbance [7]. Although two of the studies [2,6] showed that the dominant UF is involved in naming performance, the types of naming errors differed between the two studies. Therefore, how the dominant UF is involved in naming performance is still uncertain. In the present study, intraoperative stimulation was used to assist in the resection of a tumour near the dominant UF. Here, we report that the patient showed multiple different symptoms related to naming objects during intraoperative stimulation of the dominant UF that provide some insights into how the dominant UF is involved in naming objects.

2. Methods

2.1. Patient

The patient was a 39-year-old Canadian man who had come to Japan in 2003 to teach English. He graduated from a college in Canada and spoke English as a first language. Following a motorbike accident, a routine computed tomography scan detected a tumour on the left insula, temporal stem, and orbitofrontal cortex. However, brain magnetic resonance (MR) images did not show contrast enhancement, so that the tumour was suspected to be benign and was followed up annually. Three years later, the tumour seemed to be larger, and was suspected to be a low-grade astrocytoma (Fig. 1). All preoperative and postoperative neuropsychological tests and an intraoperative naming test were performed in English. He was 100 percent right-handed as measured by the Edinburgh Handedness Inventory. According to the Magnetoencephalography and thiamylal

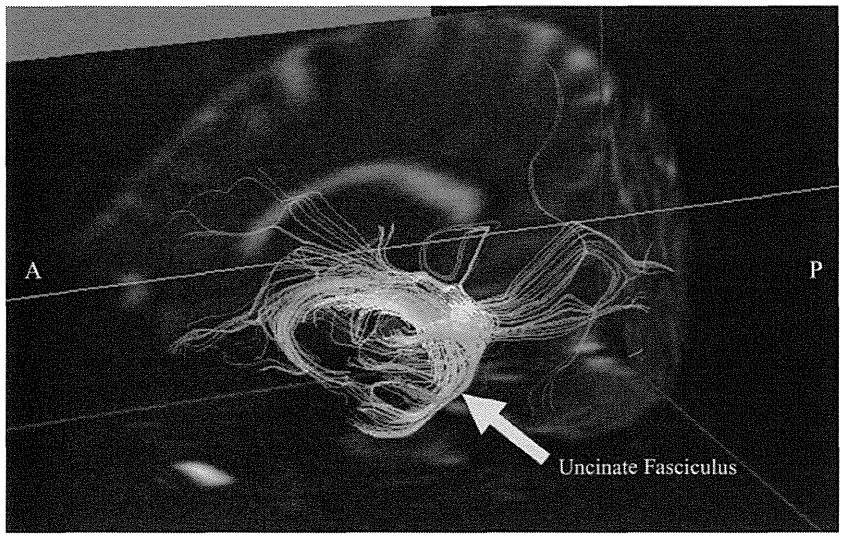

Fig. 2. Preoperative fibre tracking used to set the region of interest in the left temporal stem. The tract that is hooked at the left anterior temporal region was the left uncinate fasciculus (yellow arrow). The tract running backward is the left optic radiation. A: anterior, P: posterior.

sodium Wada Test with language tasks, his language functions were lateralised to the left hemisphere. The Wada Test also revealed that both hemispheres were involved in verbal memory. He experienced no seizure episodes or behavioural changes prior to the tumour resection. Written informed consent was obtained from the patient for publication of this report.

2.2. *Preoperative cognitive performance*

Preoperatively, the patient complained about mild word-finding difficulties only when he was talking with native English speakers on business, but his colleagues did not make any remarks about it. He scored 30/30 on the Mini-Mental State Examination (MMSE). In the Western Aphasia Battery (WAB), he scored an aphasia quotient (AQ) of 99.6, a language quotient (LQ) of 99.8, and a cortical quotient (CQ) of 99.0, respectively. These results of the examinations indicated that his cognitive performance was not impaired.

2.3. *Preoperative magnetic resonance-diffusion tensor imaging data acquisition and processing*

Preoperatively, anatomical MR images and DTIs were acquired on a 3.0 Tesla MR whole-body imager (Signa VH/i, GE medical Systems, Milwaukee, WI, USA). Three-dimensional fibre tracking (FT) based on the DTI data was performed using Volume-One and dTV software (free software by Masutani, URL: http://www.ut-radiology.umin.jp/people/masutani/dTV.htm). The UF tractography was performed using a two-region of interest (ROI) method in the same way of a previous study [8]. The seed ROIs were placed in the anterior part of the UF in the coronal plane at the level of the anterior portion of the genu of the corpus callosum that was anterior to the anterior horn of the lateral ventricle. The target ROIs were placed in the white matter in the coronal plane at the most anterior part of the temporal stem. The colour-coded maps were employed to precisely and objectively place these ROIs into the UF tracts. To determine reconstructed coronal sections at the level of the genu of the corpus callosum, a reconstructed sagittal section of the colour-coded map was employed. Figure 2 shows the left UF with the FT images.

2.4. *Intraoperative electrical stimulation*

A Stryker Navigation System (Stryker, Kalamazoo, MI, USA) was used with 1.4 mm thin-slice sagittally sectioned MR images, which the FT had been superimposed on, for the navigation. After the main mass of the tumour was resected, electrical stimulation in combination with a picture-naming task was performed under local anaesthesia to determine whether additional tumorous tissue could be resected without impairing its function. The stimulation point abutted the posterior limb of the internal capsule and was very close to the left UF (Fig. 3). An Ojemann bipolar stimulator with 5 mm spaced tips was applied to deliver a biphasic current. The electrical stimulation was 6 mA. Each

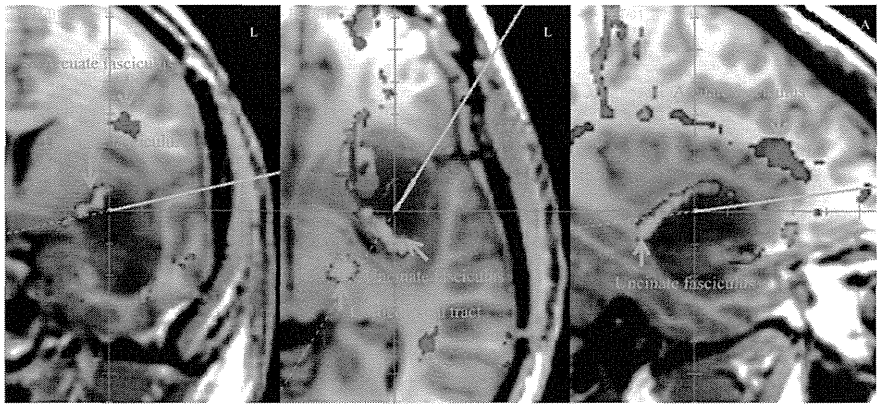

Fig. 3. Intraoperative neuronavigation pictures, in which the preoperative two-dimensional fibre tracking was projected on transaxial T1-weighted MR images (Left: a coronal image, Middle: a transaxial image, and Right: A sagittal image). The blue lines point to where the electrical stimulation with a picture-naming task was provided. L: left, A: anterior.

stimulation consisted of biphasic square wave pulses of 0.2 millisecond single phase duration at 50 Hz with the maximal train duration of five seconds. As Fig. 3 shows, we intermittently stimulated the same point at a distance of within 5 mm from the dominant UF. An electrical stimulation of 6 mA was shown to reach 5 mm from the stimulation point [9]. The electrocorticography activity was monitored to observe spontaneous or after-discharge spikes to minimise the risks of evoking a seizure by continued stimulation and to avoid the possibility of errors caused by the propagated effects of the current [2].

2.5. *Picture-naming task*

In the picture-naming task, the patient was asked to name a colour picture of an object that was on the computer screen beside his face. We prepared eight different colour pictures, which the patient could correctly name on a preoperative examination. The picture stimuli were presented repeatedly one after another in the following order: a clock, tire, banana, strawberry, pencil, umbrella, bicycle, and elephant. The picture-naming task was continuously performed while the dominant UF was being either stimulated or not stimulated. The patient was not informed when the dominant UF was being stimulated. The whole picture-naming task took approximately 10 minutes.

3. Results

3.1. *Intraoperative electrical stimulation*

We performed the picture-naming task eight times under the condition of stimulating the dominant UF. Among the eight times, the patient showed five incorrect responses. The patient stammered twice when he tried to name a picture of an umbrella and a banana respectively. The responses were considered as naming difficulty. When seeing a picture of a strawberry, the patient answered "fish", which was not in the picture stimuli. A fish and strawberry are not semantically interconnected, and the response was considered as verbal paraphasia. When the patient was shown a picture of an elephant, he answered "umbrella", which was shown two picture stimuli earlier. The response was considered as recurrent perseveration, which is an unintentional repetition of a preceding response when a new response following an interruption is expected to occur [10]. When asked a second time, he answered "umbrella" again. The response was considered as continuous perseveration, which is an inappropriate repetition of a preceding response without interruption [10]. Moreover, after producing the incorrect responses, the patient always gave the preceding incorrect response even though the stimulation had ended. The responses were considered as continuous perseveration. Except for the continuous perseveration, the patient did not produce any incorrect responses when not being stimulated.

3.2. *Postoperative course*

Since the stimulation of the dominant UF produced some naming and related disturbances, the neurosurgeons did not resect additional tissue of the dominant UF. The tumour resection was successful, so that neither chemotherapy nor radiotherapy was postoperatively given. One week after the operation, the patient

scored 25/30 on the MMSE with scoring 2/5 on the serial 7's and scoring 1/3 on the recall. Regarding to his language performance, he scored the AQ of 100, the LQ of 100, and the CQ of 99.5, respectively. The patient did not show any naming difficulty, paraphasia, and perseveration. At six weeks after the operation, his MMSE score was completely back to 30/30, and he obtained a verbal memory index of 100, a visual memory index of 126, a general memory index of 106, an attention/concentration index of 102, and a delayed memory index of 105 in the Wechsler Memory Scale-Revised. Hence, his cognitive performances were not impaired by the tumour resection.

4. Discussion

When stimulating the dominant UF with the neuronavigation system during the picture-naming task, the patient displayed naming difficulty, verbal paraphasia, and recurrent and continuous perseveration. After producing the incorrect responses and after the stimulation had ended, the patient displayed continuous perseveration.

The findings of this report, in which the dominant UF stimulation caused some deteriorations of naming performance, are consistent with the results of previous tumour resection and DTI studies [2,3]. The left UF connects to the inferior frontal lobe, which is essential for word production [11]. Dysfunction of the dominant UF appears to be the cause of the naming difficulty.

The verbal paraphasia that we observed during the dominant UF stimulation is closely related to previous studies that found phonetic paraphasia and semantic paraphasia during the dominant UF stimulation with a picture-naming task [2,6]. The dominant anterior inferior temporal lobe, to which the UF connects [1], is involved in semantic memory that is information about the concept or meaning of words and objects [12,13]. Moreover, the UF is involved in verbal planning and suppression [14]. Hence, verbal perseveration should be caused by disturbances in selection of a semantically correct word and failures to suppress the inappropriate word.

Recurrent perseveration and continuous perseveration, which were induced by the dominant UF stimulation during the picture-naming task in this case, have not previously been reported to be caused by the dominant UF stimulation. Recurrent perseveration is initiated with an unsuccessful search in semantic memory for the correct word, and then a recently heard word can be selected from short-term memory [15]. A word, which has just been articulated, should be temporarily held in working memory (WM), with which the UF is associated [16]. In this case, the stimulation must have prevented the patient from retrieving a word from semantic memory, so that the patient incorrectly must have selected another word that had been recently articulated from WM.

Continuous perseveration was observed when motor output was disturbed [10] and was associated with a failure to inhibit an appropriate response [17]. Therefore, electrical stimulation of the dominant UF, which is involved in word production [11] and motor suppression [14], could produce continuous perseveration. Although it is unclear why continuous perseveration occurred just after switching off the stimulation, it was always observed after the patient produced the incorrect responses with the stimulation. The stimulation, which was enough to produce incorrect responses, might have produced continuous perseveration.

Several issues should be considered when generalising the findings of this case report. First, we need to acknowledge that we provided the picture-naming task only eight times under the condition of stimulating the UF, so that we were unable to examine whether the same incorrect responses can be observed repeatedly. Second, the tumour seemed to shift the UF medially, so that the UF may have not been placed in the expected anatomical region. Third, whenever the intraoperative neuronavigation system is employed, the possibility of an intraoperative brain shift should be considered [18, 19] because the brain shift may result in inaccuracy of stereotactic image guidance on the preoperatively acquired brain images [18] and may reduce reliability of the neuronavigation system [19]. However, the displacements of deep tumour margins or subcortical structures are not as pronounced as those of superficial or cortical structures [19,20]. Furthermore, experienced neurosurgeons identified the tumour and differentiated the brain structures including the cortices, white matter tracts, and deep brain structures based on their anatomical knowledge. Finally, we may have failed to depict the inferior occipitofrontal fasciculus (IOFF) independently from the UF because it is very difficult to distinguish these two regions in FT images [21]. Because the UF tractography method that we used has been shown to be reliable [8], we believe that we properly depicted the UF. In addition, because our stimulation point was very close to the UF (Fig. 3) and because the electric current we applied was enough to reach 5 mm from the stimulation point, the electrical

stimulation must have reached the UF. Hence, we are confident that we properly stimulated the dominant UF instead of the IOFF.

In this case, stimulating the dominant UF caused several responses (naming difficulty, verbal paraphasia, and recurrent and continuous perseveration). These findings suggest that the dominant UF is related to multiple roles in the naming of objects.

References

[1] Catani M, Howard RJ, Pajevic S, Jones DK. Virtual *in vivo* interactive dissection of white matter fasciculi in the human brain. *Neuroimage.* 2002; 17(1): 77-94.

[2] Papagno C, Miracapillo C, Casarotti A, Romero Lauro LJ, Castellano A, Falini A, Casaceli G, Fava E, Bello L. What is the role of the uncinate fasciculus? Surgical removal and proper name retrieval. *Brain.* 2011; 134(Pt 2): 405-414.

[3] McDonald CR, Ahmadi ME, Hagler DJ, Tecoma ES, Iragui VJ, Gharapetian L, Dale AM, Halgren E. Diffusion tensor imaging correlates of memory and language impairments in temporal lobe epilepsy. *Neurology.* 2008; 71(23): 1869-1876.

[4] Pataraia E, Simos PG, Castillo EM, Billingsley-Marshall RL, McGregor AL, Breier JI, Sarkari S, Papanicolaou AC. Reorganization of language-specific cortex in patients with lesions or mesial temporal epilepsy. *Neurology.* 2004; 63(10): 1825-1832.

[5] Duffau H, Capelle L, Sichez N, Denvil D, Lopes M, Sichez JP, Bitar A, Fohanno D. Intraoperative mapping of the subcortical language pathways using direct stimulations. An anatomo-functional study. *Brain.* 2002; 125(Pt 1): 199-214.

[6] Bello L, Gallucci M, Fava M, Carrabba G, Giussani C, Acerbi F, Baratta P, Songa V, Conte V, Branca V, Stocchetti N, Papagno C, Gaini SM. Intraoperative subcortical language tract mapping guides surgical removal of gliomas involving speech areas. *Neurosurgery.* 2007; 60(1): 67-80; discussion 80-62.

[7] Duffau H, Gatignol P, Moritz-Gasser S, Mandonnet E. Is the left uncinate fasciculus essential for language? A cerebral stimulation study. *J Neurol.* 2009; 256(3): 382-389.

[8] Yasmin H, Nakata Y, Aoki S, Abe O, Sato N, Nemoto K, Arima K, Furuta N, Uno M, Hirai S, Masutani Y, Ohtomo K. Diffusion abnormalities of the uncinate fasciculus in Alzheimer's disease: Diffusion tensor tract-specific analysis using a new method to measure the core of the tract. *Neuroradiology.* 2008; 50(4): 293-299.

[9] Kamada K, Todo T, Ota T, Ino K, Masutani Y, Aoki S, Takeuchi F, Kawai K, Saito N. The motor-evoked potential threshold evaluated by tractography and electrical stimulation. *J Neurosurg.* 2009; 111(4): 785-795.

[10] Sandson J, Albert ML. Varieties of perseveration. *Neuropsychologia.* 1984; 22(6): 715-732.

[11] Schuhmann T, Schiller NO, Goebel R, Sack AT. The temporal characteristics of functional activation in Broca's area during overt picture naming. *Cortex.* 2009; 45(9): 1111-1116.

[12] Damasio H, Grabowski TJ, Tranel D, Hichwa RD, Damasio AR. A neural basis for lexical retrieval. *Nature.* 1996; 380(6574): 499-505.

[13] Patterson K, Nestor PJ, Rogers TT. Where do you know what you know? The representation of semantic knowledge in the human brain. *Nat Rev Neurosci.* 2007; 8(12): 976-987.

[14] Hornberger M, Geng J, Hodges JR. Convergent grey and white matter evidence of orbitofrontal cortex changes related to disinhibition in behavioural variant frontotemporal dementia. *Brain.* 2011; 134(Pt 9): 2502-2512.

[15] Shindler AG, Caplan LR, Hier DB. Intrusions and perseverations. *Brain Lang.* 1984; 23(1): 148-158.

[16] Charlton RA, Barrick TR, Lawes IN, Markus HS, Morris RG. White matter pathways associated with working memory in normal aging. *Cortex.* 2010; 46(4): 474-489.

[17] Possin KL, Filoteo JV, Roesch SC, Zizak V, Rilling LM, Davis JD. Is a perseveration a perseveration? An evaluation of cognitive error types in patients with subcortical pathology. *J Clin Exp Neuropsychol.* 2005; 27(8): 953-966.

[18] Benveniste RJ, Germano IM. Correlation of factors predicting intraoperative brain shift with successful resection of malignant brain tumors using image-guided techniques. *Surg Neurol.* 2005; 63(6): 542-548; discussion 548-549.

[19] Reinges MH, Nguyen HH, Krings T, Hutter BO, Rohde V, Gilsbach JM. Course of brain shift during microsurgical resection of supratentorial cerebral lesions: Limits of conventional neuronavigation. *Acta Neurochir (Wien).* 2004; 146(4): 369-377; discussion 377.

[20] Hastreiter P, Rezk-Salama C, Soza G, Bauer M, Greiner G, Fahlbusch R, Ganslandt O, Nimsky C. Strategies for brain shift evaluation. *Med Image Anal.* 2004; 8(4): 447-464.

[21] Makris N, Papadimitriou GM, Sorg S, Kennedy DN, Caviness VS, Pandya DN. The occipitofrontal fascicle in humans: A quantitative, *in vivo*, DT-MRI study. *Neuroimage.* 2007; 37(4): 1100-1111.

INVITED PAPER Special Section on SQUID & its Applications

Clinical Application of Neuromagnetic Recordings: From Functional Imaging to Neural Decoding

Masayuki HIRATA[†a)] *and* Toshiki YOSHIMINE[†], *Nonmembers*

SUMMARY Magnetoencephalography (MEG) measures very weak neuromagnetic signals using SQUID sensors. Standard MEG analyses include averaged waveforms, isofield maps and equivalent current dipoles. Beamforming MEG analyses provide us with frequency-dependent spatiotemporal information about the cerebral oscillatory changes related to not only somatosensory processing but also language processing. Language dominance is able to be evaluated using laterality of power attenuation in the low γ band in the frontal area. Neuromagnetic signals of the unilateral upper movements are able to be decoded using a support vector machine.

key words: *magnetoencephalography, oscillation, neuroimaging, beamformer, neural decoding*

1. Introduction

Intensity of neuromagnetic signals ranges from 10^{-14} tesla (T) to 10^{-12} T, which is approximately billionth part of earth's magnetism and millionth part of that of magnetic noises in cities. Magnetoencephalography (MEG) measures such very weak neuromagnetic signals directly related to intracellular electrical currents caused by neuronal activities, so that MEG enables us to detect neural activities with temporal resolution as high as millisecond order [1]. SQUID sensors are used as neuromagnetic sensors, which have sufficient sensitivity as high as approximately 10 fT/$\sqrt{\text{Hz}}$ (white noise). MEG estimates neural current generators more precisely than electroencephalography (EEG). Because magnetic reluctance of the body tissues is uniform, neuromagnetic signals fit better with simple conductance models of the skull for analyses, whereas electric conductance of the body tissues is not uniform. Utilizing the precision, MEG is used for neuroscientific researches and neurological evaluations such as functional neuroimaging and evaluation of epileptic foci [2]. Most recently, neural decoding techniques have been introduced in the field of MEG to facilitate the effectiveness of neurorehabilitation [3].

In this paper, we describe the recent progress in our MEG research on clinical application regarding functional neuroimaging and neural decoding based on neuromagnetic recordings.

Manuscript received July 23, 2012.
Manuscript revised October 31, 2012.
[†]The authors are with the Department of Neurosurgery, Osaka University Medical School, Suita-shi, 565-0871 Japan.
a) E-mail: mhirata@nsurg.med.osaka-u.ac.jp
DOI: 10.1587/transele.E96.C.313

2. Backgrounds

2.1 Cerebral Oscillatory Changes

Synchronous oscillations in specific frequency bands such as alpha waves are well known as basic brain rhythms. These basic rhythms change signal power due to brain activation. Event-related desynchronization (ERD) is an attenuation of the oscillation amplitude of a specific frequency band that occurs in relation to specific neural activities [4]. The opposite phenomenon, event-related synchronization (ERS), is an increase in that amplitude [5].

Synchronous oscillations can be measured using EEG, MEG and electrocorticography (ECoG) which is neural activities recorded from electrodes directly placed on the brain surface. Figure 1 shows the time-frequency spectrograms of ECoGs during right hand grasping. The ECoGs are recorded from grid electrodes placed over the left sensorimotor areas of the human brain. ERDs are observed in the 8–25 Hz (α and β bands) over the sensorimotor areas broadly, whereas ERSs are observed in the 50–200 Hz (high γ band) in the sensorimotor areas more focally. Regarding time domain also, ERDs occur 500–1000 ms prior to muscle contraction and sustained even after the end of muscle contraction, whereas ERSs occurs more strictly during muscle contraction. ERS in the high γ band is known to reflect functional localization of the brain better than ERD in the α and β bands. These oscillatory changes during movements are called as movement-related cerebral oscillatory changes. Cerebral oscillatory changes are observed not only during movements, but also during language activities, sensory processing and mental concentration. ECoG provides us with precise neural activities directly from brain surface electrodes, but needs brain surgery. MEG is noninvasive as well as precise in functional localization.

2.2 Conventional Methods for MEG Analyses

Averaged waveforms, isomagnetic fields, and equivalent current dipoles (ECDs) are conventional methods for MEG analyses. Averaged waveforms are used to detect weak neuromagnetic activities by improving signal-to-noise ratio by averaging time-locked signals. They are appropriate for detecting relatively short latency activities less than several hundred milliseconds. Isomagnetic fields estimate rough

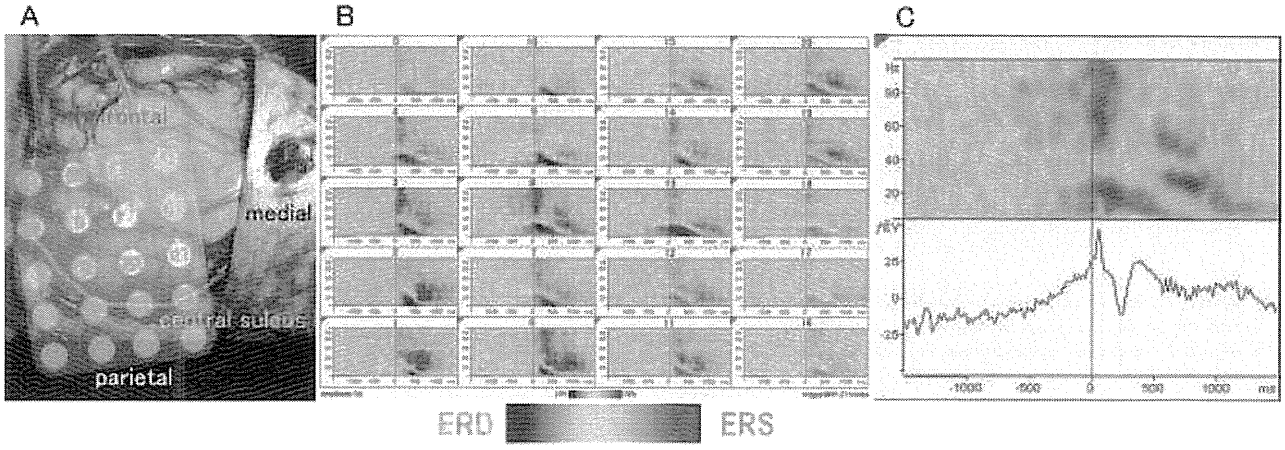

A. Electrode configuration on the brain. B. Time frequency spectrograms of the grid electrodes. ERS in the γ band is focally distributed, whereas ERD in the α and β bands is broadly distributed. C. A time-frequency spectrogram (upper) and a cortical potential (lower) of electrode 8.

Fig. 1 Cerebral oscillatory changes recorded from brain surface grid electrodes.

localization of an electric current generator from the distribution of inflow and outflow magnetic fields. An ECD estimates the localization, magnitude and direction of an electric current generator quantitatively as an electric dipole equivalent to the distribution of inflow and outflow magnetic fields based on the Biot-Savart law. These methods enable us to grasp neural activities based on relatively simple principles, while they have several disadvantages. First, for example, when we detect evoked responses to specific stimuli using averaged waveforms, averaging process improves signal-to-noise ratio of the short latency responses. In contrast, high frequency components tend to be lost in the late latency, because the phases of neural responses in the latency might vary from a stimulus to a stimulus, which is a typical characteristic of biological responses. Second, an ECD estimates an electric current generator as a point. However, higher brain functions such as language and cognitive functions activate multiple brain areas simultaneously. ECD has some difficulty in estimating such complex spatial distribution.

2.3 Adaptive Beamformer

To overcome these issues, various methods to estimate complex spatial distribution of neural activities have been introduced. Adaptive beamformer is a spatial noise filtering method and it is used to estimate complex spatial distribution of neural activities from unaveraged MEG signals [6]. Compared with conventional methods, adaptive beamformer takes advantages as follows: 1) high spatial resolution by statistical spatial filtering, 2) ability to elucidate the activities in the high frequency bands and in the late latency without averaging.

Adaptive beamformer assumes the matrix of each voxel within region of interest (ROI) as a virtual sensor array, and estimates source power for each voxel by minimizing signal power due to all other sources. The spatiotemporal MEG signal $\mathbf{M}$ can be written in matrix form:

$$\mathbf{M} = [m_{ik}] \quad (1)$$

$i = 1 \sim M, \quad k = 1 \sim K$

M: number of sensors

K: number of time samples

m_{ik} is a function of the current $\mathbf{J}$ throughout the head volume Ω:

$$m_{ik} = \int_{\Omega} \mathbf{J}_k(\mathbf{r}) \cdot \mathbf{G}_i(\mathbf{r}) dr^3 + n_{ik} \quad (2)$$

where Green's functions G are used to represent the sensitivity of each sensor to current flow, and n is the instantaneous noise at sensor i. The sensor variance is represented by diagonal matrix $\sum$:

$$\sum = \begin{bmatrix} \sigma_1^2 & & 0 \\ & \ddots & \\ 0 & & \sigma_M^2 \end{bmatrix} \quad (3)$$

The source power estimate S_θ is:

$$S_\theta^2 = [\mathbf{H}_\theta^T \ \mathbf{M}]^2 \quad (4)$$

$\mathbf{H}$: a vector of M beamforming coefficients

$\mathbf{M}$: the signal space vector

θ: the target within brain.

The source noise variance is estimated:

$$\sigma_\theta^2 = \mathbf{H}_\theta^T \sum \mathbf{H}_\theta \quad (5)$$

Two additional constraints are required for solution of the beamforming coefficients. First, power S must be a measure of source and not signal:

$$\mathbf{H}_\theta^T \mathbf{G}_\theta \equiv 1 \quad (6)$$

Second, uncorrelated noise will appear in the source power

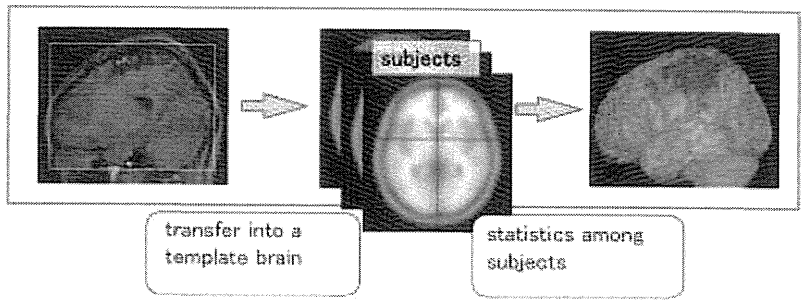

Fig. 2 A conceptual diagram of group analyses.

estimate of Eq. (5). This constraint sets an upper limit on the noise:

$$\sigma_\theta \leq \xi_\theta \tag{7}$$

The beamformer coefficients are computed by minimizing source power (Eq. (4)):

$$S_\theta^2 = \mathbf{H}_\theta^T \mathbf{C} \mathbf{H}_\theta \tag{8}$$

$\min \mathbf{H}$

C: the covariance matrix.

Thus, the source power estimate solution becomes:

$$S_\theta^2 = \left[\mathbf{G}_\theta^T \left[\mathbf{C} + \mu \sum \right]^{-1} \mathbf{G}_\theta \right]^{-1} \tag{9}$$

μ: a Backus-Gilbert regularization parameter.

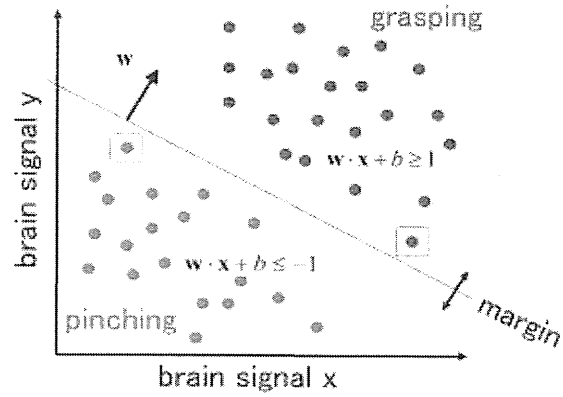

Fig. 3 A conceptual diagram of a support vector machine.

2.4 Group Analyses

We introduced group analyses to obtain common brain activities among subjects eliminating inter-individual difference (Fig. 2) [7].

Group statistical maps are generated by normalizing the individual results to standard space and then combining these results across subjects for each frequency band. First, each individual's anatomical MRI is resliced to the same orientation and position as the beamforming MEG results and statistical parametric mapping is used to find the transformation matrix from this functional space into the Montreal Neurological Institute (MNI) template. The transformation matrix is then applied to each of the beamforming MEG results in each frequency band, and for each subject. A permutation test is used to generate group statistical maps over each voxel in the standard brain using statistical non-parametric mapping (SnPM; Wellcome Department of Imaging Neuroscience, London, UK). Analysis at the voxel level was performed using a pseudo-T-statistic incorporating variance smoothing with a Gaussian kernel of width 8 mm. These group statistical maps were then thresholded at $p < 0.001$ (corrected), and superimposed on the MNI template brain using mri3dX (CUBRIC, Cardiff, UK).

2.5 Neural Decoding

Neural decoding is a method to infer the content of behavior or cognition from brain signals alone. Progress of functional brain researches has enabled us to neural decoding. Various methods are used for neural decoding. Here, we show a support vector machine (SVM) [8], which we use to decode neuromagnetic signals during upper hand and arm movements in our study [9].

An SVM is a learning machine which is often used for pattern recognition. It constructs a hyperplane or set of hyperplanes in a high- or infinite-dimensional space, which can be used for classification, regression, or other tasks. Intuitively, a good separation is achieved by the hyperplane that has the largest distance to the nearest training data point of any class, so-called functional margin, since in general the larger the margin the lower the generalization error of the classifier (Fig. 3). An SVM takes a set of input data and predicts, for each given input, which of multiple possible classes forms the input, making it a non-probabilistic classifier. Given a set of training examples, each marked as belonging to one of multiple categories, an SVM training algorithm builds a model that assigns new examples into one category. An SVM model is a representation of the examples as points in space, mapped so that the examples of the separate categories are divided by a clear gap that is as wide as possible. New examples are then mapped into that same space and predicted to belong to a category based on which side of the gap they fall on.

3. Neuromagnetic Imaging of Cerebral Oscillatory Changes

3.1 Somatosensory Processing

Typical neuromagnetic somatosensory responses are observed when we stimulate major peripheral nerves of the body. We measured neuromagnetic responses using a whole head type axial gradiometer equipped with 64 SQUID sensors. Figure 4 shows the averaged waveforms of the somatosensory responses of all 64 SQUID sensors for 100 electrical stimuli to the right median nerve at the wrist in a healthy subject. Clear responses are observed in 20 ms, 26 ms, 39 ms and 51 ms after the stimuli. Isomagnetic field maps show clear inflow and outflow of neuromagnetic fields. A current dipole equivalent to the magnetic field at 20 ms after the stimuli is localized just in the contralateral postcentral gyrus. The postcentral gyrus is well known as the primary somatosensory area, where somatosensory processing such as touch and vibration sensation of the body.

Beamformer analyses provide us with additional information about spatiotemporal distribution of neural processing. Beamformer analyses show the distributed ERS in the contralateral somatosensory area in the high γ band (50–200 Hz) as well as the ERDs in the bilateral somatosensory areas in the α (8–13 Hz) and β (13–25 Hz) bands (Fig. 5) [10]. These ERDs and ERS are suggested to reflect inhibitory and excitatory neural activities related to somatosensory processing.

3.2 Language Processing

Compared to somatosensory processing, neuromagnetic responses to linguistic stimuli are more complex. We use a silent reading task to avoid the noise contamination due to muscle contraction during phonation. A 3-character hiragana word was presented on a display for 3 seconds. Subjects are instructed to silently read the words once as soon as the words were presented. A total of 100 words were presented serially every 6 seconds. Figure 6A shows the averaged waveforms of neuromagnetic responses of all 64 SQUID sensors for visually-presented hiragana words in a healthy subject. They have later latency components and isofield maps indicate more complex inflow and outflow distribution than those of somatosensory processing (Fig. 6B). Single ECD analyses managed to localize an ECD until 330 ms, but represented only part of the complex neuromagnetic fields. Multiple ECD analyses failed to localize stable ECDs with sufficient goodness of fit.

Beamformer analyses provide us with complex spatial distribution of cerebral oscillatory changes during silent reading. Figure 7 shows the result of group analysis for 14 healthy right-handed subjects. It is noteworthy that the spa-

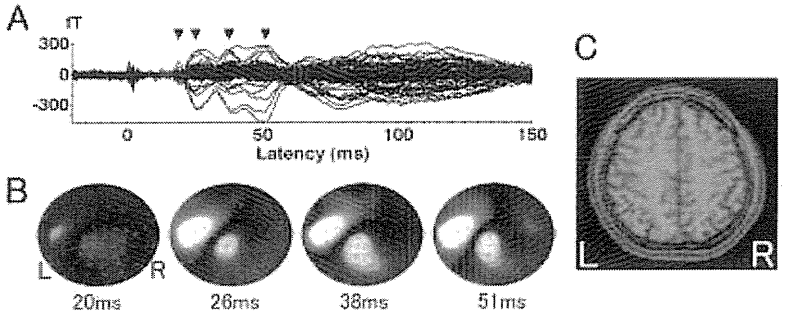

Neuromagnetic responses to the right median nerve electrical stimulation
A. Averaged waveforms
B. Isomagnetic fields
Inflows are indicated in red and outflows in blue.
C. An equivalent current dipole

Fig. 4 Standard MEG analyses.

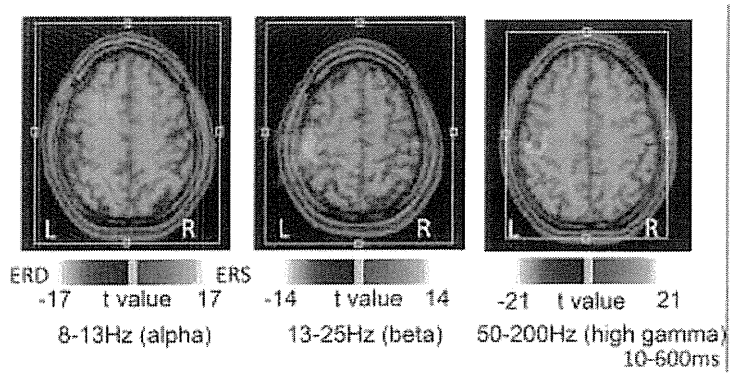

Fig. 5 Cerebral oscillatory changes during somatosensory stimulation revealed by beamforming MEG analyses.

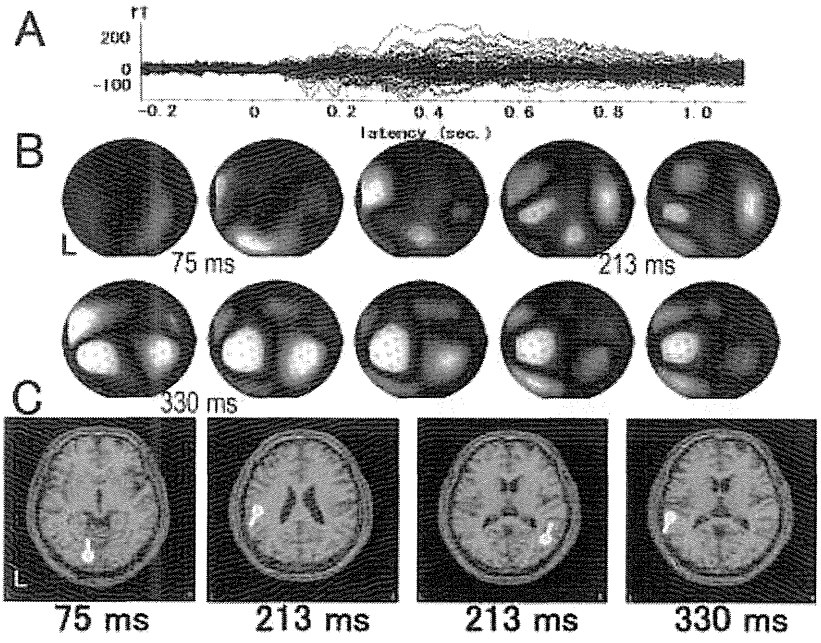

A. Averaged waveforms
B. Isofield maps
C. Equivalent current dipoles (ECDs)
Compared to somatosensory responses, averaged waveforms have late latency components and isofield maps indicate complex inflow and outflow distribution. Single ECD represents only part of the complex neuromagnetic fields. However, multiple ECD analyses failed to localize stable ECDs with sufficient goodness of fit.

Fig. 6 Neuromagnetic responses during silent reading.

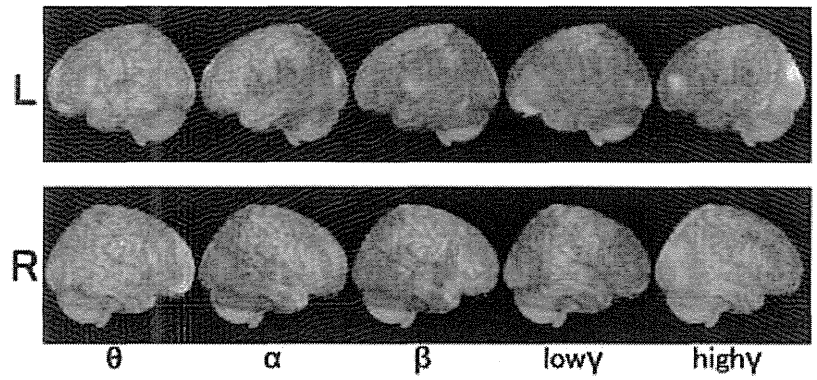

Beamforming MEG group analyses well represent frequency-dependent complex spatial distribution of cerebral oscillatory changes during silent reading. ERDs in the α band distributed in the receptive language area, whereas ERDs in the low γ band distributed in the expressive language area.

Fig. 7 Spatial distribution of cerebral oscillatory changes during silent reading revealed by beamforming MEG group analyses for 14 healthy right-handed subjects.

tial distribution is dependent on the frequency bands of the oscillatory changes. ERDs in the α band distributed in the posterior (receptive) language area, whereas ERDs in the low γ band distributed in the frontal (expressive) language area [7]. In addition, we found that the left and right lateralization of ERD in the frontal area in the low γ band well corresponds to language dominance [11]. Using this property, we established the method to evaluate language dominance noninvasively with beamforming MEG analyses. Compared to the standard but invasive method for language dominance (the Wada test) which requires the injection of anesthetic agents intra-arterially at the carotid artery, the consistency is approximately 85% [7]. Beamforming MEG analysis is considered to be an alternative to the Wada test in selected cases. Figure 9 shows an example of language dominance evaluated by this method.

Sliding time window analyses of beamforming MEG revealed the temporal profiles of cerebral oscillatory changes during silent reading (Fig. 8) [12]. We found that the transient ERS first occurred in the occipital visual area, then in the temporo-occipital language areas, and finally propagated to the frontal language areas. This transient θ (8–13 Hz) ERS was followed by α ERDs in the temporo-occipital language areas and low γ ERDs in the frontal language areas. High γ ERS was found in the occipital lobe, which reflects visual processing. It seems that transient θ ERS reflects serial processing while α and low γ ERDs reflect parallel neural processing.

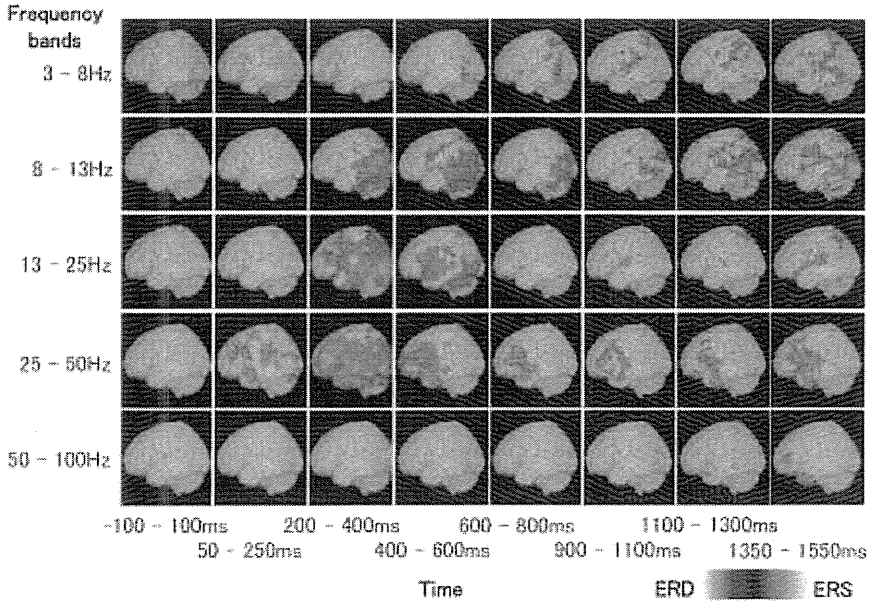

Sliding time window analyses of beamforming MEG reveal the temporal profiles of cerebral oscillatory changes during silent reading. Note that transient θ ERS precedes α to low γ ERDs. High γ ERS was found in the occipital lobe, which reflects visual processing.

Fig. 8 Time course of spatial distribution of cerebral oscillatory changes during silent reading revealed by beamforming MEG group analyses.

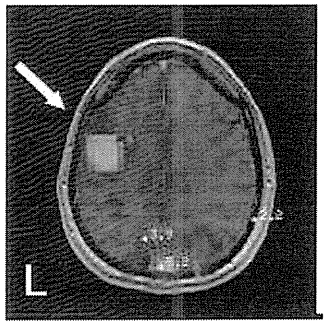

ERD is indicated by blue color area.

Fig. 9 Language dominance estimated by left and right lateralization of ERD in the frontal area in the low γ band.

4. Neural Decoding of Upper Limb Movements Using Single Trial Neuromagnetic Signals

We investigated neural decoding of upper limb movements using single trial neuromagnetic signals. Neuromagnetic activities were recorded in 9 healthy subjects during 3 types of unilateral upper limb movements. The movement types were inferred by a SVM. A one-way analysis of variance (ANOVA) was performed to reveal the spatiotemporal differences in the magnetic fields among the three movements. Significant F values in all MEG channels were calculated using the same parameters used for calculating the time course of the decoding accuracy. The topographies of the F values were delineated on a map of MEG sensors to determine which channels exhibited significant differences in neuromagnetic activities among movements.

The movement types were successfully predicted with an average accuracy of 66 ± 10% (chance level: 33.3%) using neuromagnetic activity during a 400-ms interval (−200 ms to 200 ms from movement onsets) [13]. Figure 10A shows the temporal profiles of averaged waveforms of normalized magnetic fields and decoding accuracy in a representative subject. Three peaks of decoding accuracy were found corresponding to the peaks of averaged waveforms of neuromagnetic fields. Topography of F values showed that high F values distributed over the parietal and sensorimotor areas (Fig. 10B). The decoding accuracy was significantly correlated with amplitude of normalized neuromagnetic fields [9].

Our results indicate that the three types of unilateral upper limb movement can be inferred with high accuracy by detecting differences in movement-related brain activity in the parietal and sensorimotor areas.

5. Conclusion

We reviewed the recent progress in our MEG research on clinical application regarding functional neuroimaging and neural decoding using neuromagnetic recordings. Beamforming MEG analyses provide us with frequency-dependent spatiotemporal information about the cerebral oscillatory changes related to not only somatosensory processing but also language processing. Language dominance is able to be evaluated using laterality of the low γ ERD in the frontal area. Neuromagnetic signals of the unilateral upper movements are able to be decoded using a SVM.

Acknowledgments

This work was supported in part by Grants-in-Aid for Scientific Research (22390275, 23390347, 24000012, 24650106)

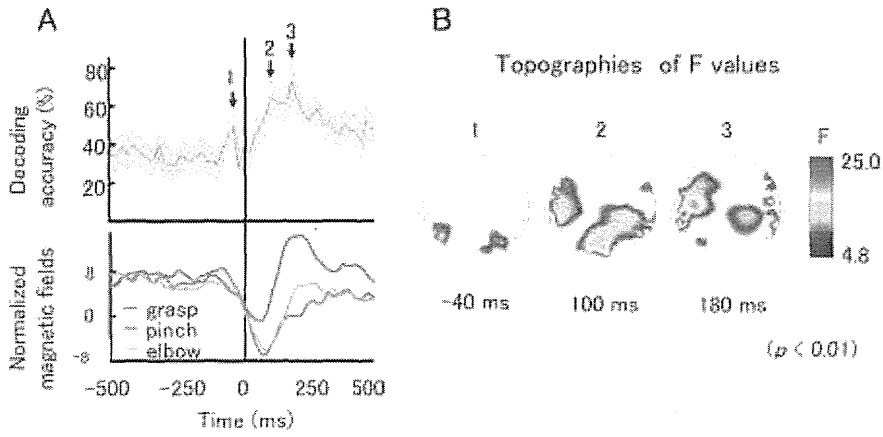

A. Temporal profiles of averaged waveforms of normalized magnetic fields and decoding accuracy in a representative subject.
B. Topography of F values among three movements

Fig. 10 Neural decoding of upper limb movements using single trial neuromagnetic signals.

from JSPS, by Health and Labour Sciences Research Grants (23100101) and by the Strategic Research Program for Brain Sciences of MEXT.

References

[1] Z.N. Lu, and L. Kaufman, ed., Magnetic source imaging of the human brain, Lawrence Erlbaum Associates, Publishers, New Jersey, 2003.
[2] H. Stefan, C. Hummel, G. Scheler, A. Genow, K. Druschky, C. Tilz, M. Kaltenhauser, R. Hopfengartner, M. Buchfelder, and J. Romstock, "Magnetic brain source imaging of focal epileptic activity: A synopsis of 455 cases," Brain: A Journal of Neurology, vol.126, no.Pt11, pp.2396–2405, Nov. 2003.
[3] N. Birbaumer and L.G. Cohen, "Brain-computer interfaces: Communication and restoration of movement in paralysis," J. Physiol, vol.579, no.Pt3, pp.621–636, March 2007.
[4] G. Pfurtscheller and A. Aranibar, "Event-related cortical desynchronization detected by power measurements of scalp EEG," Electroencephalogr Clin Neurophysiol, vol.2, pp.817–826, 1977.
[5] G. Pfurtscheller, "Event-related synchronization (ERS): An electrophysiological correlate of cortical areas at rest," Electroencephalogr Clin Neurophysiol, vol.83, pp.62–69, 1992.
[6] S.E. Robinson and J. Vrba, "Functional neuro-imaging by synthetic aperture magnetometry (SAM)," in Recent Advances in Biomagnetism, ed. T. Yoshimoto, M. Kotani, H. Karibe, and N. Nakasato, pp.302–305, Tohoku Univ. Press, 1999.
[7] M. Hirata, T. Goto, G. Barnes, Y. Umekawa, T. Yanagisawa, A. Kato, S. Oshino, H. Kishima, N. Hashimoto, Y. Saitoh, N. Tani, S. Yorifuji, and T. Yoshimine, "Language dominance and mapping based on neuromagnetic oscillatory changes: Comparison with invasive procedures," J. Neurosurg, vol.112, no.3, pp.528–538, March 2010.
[8] Y. Kamitani and F. Tong, "Decoding the visual and subjective contents of the human brain," Nat Neurosci, vol.8, no.5, pp.679–685, May 2005.
[9] H. Sugata, T. Goto, M. Hirata, T. Yanagisawa, M. Shayne, K. Matsushita, T. Yoshimine, and S. Yorifuji, "Movement-related neuromagnetic fields and performances of single trial classifications," Neuroreport, vol.23, no.1, pp.16–20, 2012.
[10] M. Hirata, A. Kato, M. Taniguchi, H. Ninomiya, D. Cheyne, S.E. Robinson, M. Maruno, E. Kumura, R. Ishii, N. Hirabuki, H. Nakamura, and T. Yoshimine, "Frequency-dependent spatial distribution of human somatosensory evoked neuromagnetic fields," Neurosci. Lett., vol.318, pp.73–76, 2002.
[11] M. Hirata, A. Kato, M. Taniguchi, Y. Saitoh, H. Ninomiya, A. Ihara, H. Kishima, S. Oshino, T. Baba, S. Yorifuji, and T. Yoshimine, "Determination of language dominance with synthetic aperture magnetometry: Comparison with the Wada test," Neuroimage, vol.23, pp.46–53, 2004.
[12] T. Goto, M. Hirata, Y. Umekawa, T. Yanagisawa, M. Shayne, Y. Saitoh, H. Kishima, S. Yorifuji, and T. Yoshimine, "Frequency-dependent spatiotemporal distribution of cerebral oscillatory changes during silent reading: A magnetoencephalograhic group analysis," NeuroImage, vol.54, no.1, pp.560–567, Jan. 2011.
[13] H. Sugata, T. Goto, M. Hirata, T. Yanagisawa, M. Shayne, K. Matsushita, T. Yoshimine, and S. Yorifuji, "Neural decoding of unilateral upper limb movements using single trial MEG signals," Brain Res, vol.1468, pp.29–37, June 2012.

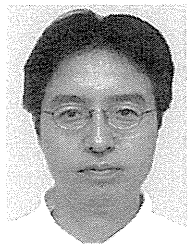

Masayuki Hirata B.S., M.S. and M.D. and Ph.D. graduated from Faculty of Engineering, The University of Tokyo in 1985 and Osaka University Medical School in 1994. Board-certified neurosurgeon specialized in functional neurosurgery. He was promoted to a Specially-Appointed Associate Professor, Dept. of Neurosurgery, Osaka University Medical School serving as a leader of neural engineering group.

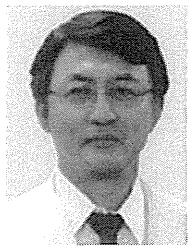

Toshiki Yoshimine M.D., Ph.D. graduated from Osaka University Medical School in 1975. Board-certified neurosurgeon, specialized in brain tumor and epilepsy surgery. He is a Director, Japan Neurosurgical Society, and Neurotrauma Committee Member, World Federation of Neuro-surgical Societies (WFNS). He has been a research fellow in Mayo Clinic in 1980–1983, a visiting professor in University of Mainz in 1995. He currently serves as Professor and Chairman, Dept. of Neurosurgery, Osaka University Medical School and Director, Medical Center for Translational Research, Osaka University Hospital.

皮質脳波を用いたブレイン・マシン・インターフェースによる身体機能障害の代替

大阪大学大学院医学系研究科脳神経外科学
特任准教授　平田雅之、教授　吉峰俊樹

1．皮質脳波BMIの概要

1-1.皮質脳波BMIの特徴、既存技術の問題点

ブレイン・マシン・インターフェース(brain machine interface：BMI)とは、脳信号を計測・解析して、運動や発話の内容を推定し、ロボットアームやコンピュータ等の外部機器を制御することにより機能を代替・支援する技術である[1](図1)。身体障害者や高齢者など要介護者の障害された機能を補填・代替する技術として期待されている。

身体障害者に対する機能代替・支援方法としては筋電信号や眼球運動を~~利用するものがある~~。運動機能の支援装置としては、切断肢に対する筋電信号を用いた義手や麻痺肢に対するアシストスーツ[2]などがある。また意思伝達の支援装置としては、筋力低下患者に対しては押しボタン等のON/OFFスイッチによる意思伝達装置があり、また完全四肢麻痺であるが眼球運動が残存している閉じ込め症候群の患者に対しては注視点検出による意思伝達装置がある。これらの装置は、完全もしくは重度麻痺で筋活動がないもしくは強い場合や、眼球も動かない場合には利用困難となる。

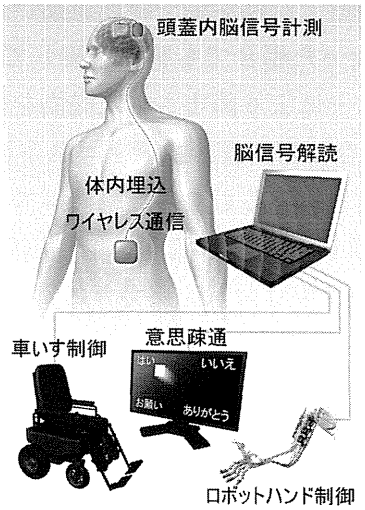

図1　ブレイン・マシン・インターフェース(BMI)の概念図(体内埋込型BMIを示す。)

BMIも手術の有無により非侵襲型、侵襲型に大きく二つに分類され、使用する脳信号も様々である（表1）。非侵襲型は脳波や近赤外分光法、機能的MRIなど非侵襲的脳信号計測を用い、その非侵襲性を活かして簡易的なBMIやニューロリハビリテーションへの応用を目指して研究が行われている[3)～5)]。これに対して侵襲型はその高性能を活かして体内埋込による身体障害者に対する機能代替への応用を目指して研究が行われている[6)、7)]。侵襲型は電極設置手術を必要とし、脳表面に皿状電極を留置する皮質脳波BMIと、大脳実質に微小針電極を刺入する刺入電極BMIに分類される[1)]。BMIの応用においては脳信号の特徴を踏まえて、用途に応じてどの脳信号を用いるかを決めることが重要である。

表1　BMIに用いられる脳信号

	計測範囲	計測対象	空間分解能	時間分解能	時間遅れ	侵襲性	長期計測安定性	可搬性
fMRI	◎全脳	脳血流	○3-5mm	× 4-5秒	× 4-5秒	◎なし	○高	× なし
NIRS	◎全域	脳血流	× 2cm	× 4-5秒	× 4-5秒	◎なし	○高	○良
EEG	◎全域	脳活動	× 3-4cm	○ 1ms	◎なし	◎なし	○高	○良
MEG	◎全域	脳活動	△5-10mm	◎0.1ms	◎なし	◎なし	○高	× なし
ECoG	○10x10cm^2	脳活動	○2-3mm	◎0.1ms	◎なし	△中	◎高	◎良
LFP	○ 5x5mm^2	脳活動	○ 1mm	◎0.1ms以下	◎なし	× 高	△中	◎良
spike	○ 5x5mm^2	脳活動	◎0.2mm	◎0.1ms以下	◎なし	× 高	× 低	◎良

注) NIRS: near infrared spectroscopy (近赤外分光法), EEG: electroencephalogram (脳波), MEG: magnetoencephalography (脳磁図), ECoG: electrocorticogram (皮質脳波), LFP: local field potential (局所集合電位), spike (神経発火活動)

1-2.競合技術との優位性

筋電義手や従来の意思伝達装置では筋活動や眼球運動が殆どなくなると利用することが困難であるが、これらがなくなった場合でも脳が機能している場合には、BMI技術を用いれば脳信号を計測・解読することにより障害された機能を代替・支援することが可能になる。図2に機能代替に関する既存技術・競合技術とコストの関係を示す。筋電信号や頭皮脳波等既存の非侵襲センサ技術を用いるものは一般にコストが低く、重症度の軽い障害者に向いているのに対して、皮質脳波や刺入電極を用いる侵襲的センサを用いるものに関してはコストが高いが、重症の障害者にも使用できる。またBMIにおいても、頭皮脳波を用いた非侵襲BMIは手術を必要としないが性能は手術を必要とする侵襲BMIには及ばない。同じ侵襲型BMIの中でも、大脳実質に微小針電極を刺入して神経細胞のspike活動を利用する刺入針電極BMIは性能は最も高いが、大脳実質に微小ながらも侵襲を加える点で安全性で皮質脳波BMIに及ばない。また刺入針電極BMIは、長期になると慢性組織反応により刺入部周囲に瘢痕形成が生じ、計測効率が低下し、性能が低下するという欠点もある。こ

れらの点を総合的に踏まえると、皮質脳波BMIは電極留置手術を必要とするものの、性能は高く、長期安定性も高く、医療応用には適した方法と考えられる。

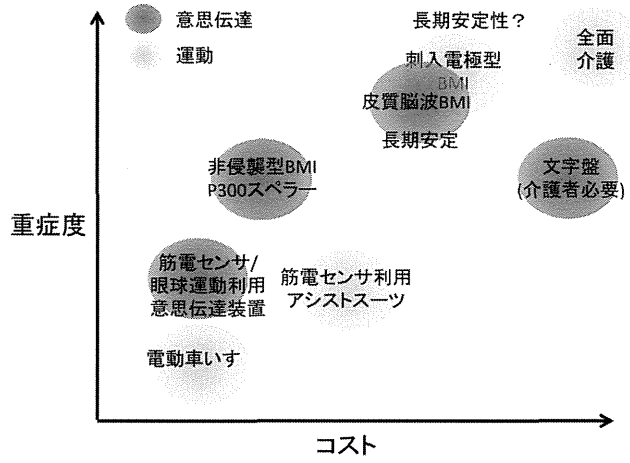

図2　機能代替に関する 既存技術・競合技術とコストの関係

2．研究開発状況と研究課題

ここでは我々が研究開発している皮質脳波BMIの研究開発状況と研究課題について述べる。刺入電極BMIもほぼ同様の研究開発段階にあると考えて良い。皮質脳波BMIの研究開発は大きく、運動・意思伝達の解読・制御システムの研究開発と、ワイヤレス体内埋込装置の研究開発に分けられる。

2-1.運動・意思伝達の解読・制御システム

運動・意思伝達の解読・制御システムに関しては、現在、皮質脳波を用いてロボットアームのリアルタイム操作、意思伝達装置の操作が可能となった[6]。最近では重症のALS患者を対象に臨床研究を開始しており、3週間、脳表電極を埋め込み、運動・意思伝達に成功している。(H25年4月11日、NHK「おはよう日本」で報道：http://www.nhk.or.jp/ohayou/marugoto/2013/04/0411.html)。

我々が開発した解読・制御アルゴリズムを図3に示す[6)、8)、9)]。最初に、運動時の皮質脳波を計測し、大脳の一次運動野に留置した脳表電極から皮質脳波を計測し、0.2秒毎に解読・制御をリアルタイムに繰り返す。まずガウス過程回帰という方法により、新たに計測した脳信号があらかじめ学習しておいた脳信号のパターンとどれくらい似通っているかを相互情報量で評価する。ガウス過程回帰の相互情報量が閾値を超えた場合にのみ、その脳信号は運動時の脳信号であると判定して、サポートベクターマシンというパターン認識の方法を用いて、運動内容を推定する。最後に、推定した運動内容にもとづいてロボットアー

ムを動かすが、遷移状態という概念を用いる。つまり、「握る」という動きであれば、「握る」という解読結果が~~など~~も連続して続いた時にのみ、ロボットアームに「開く」の姿勢から、「握る」の姿勢に段階的に徐々に姿勢を変えるように設定されている。

また運動内容解読に有用な皮質脳波の生理学的特徴量を調べた。その結果、場所としては一次運動野、特に中心溝と呼ばれる脳のしわの中の一次運動野の脳信号が有用であること[10]、また脳信号の周波数帯域としてはhigh γ帯域と呼ばれる高周波帯域の皮質脳波が運動内容推定に有用であることが明らかになった[11]。

今後の研究課題としては、ロボットアーム操作に関しては現在、手関節に関して~~現在、~~握る・開く・つまむ3種の動き、肘関節に関して曲げる・伸ばすの2種の動きを同時独立に解読・制御できるが、今後は肩関節の動きも加えて、腕を伸ばして物体を掴み、口元まで持って行く動作の実現など、より解読・制御の実用性を向上させる必要がある。

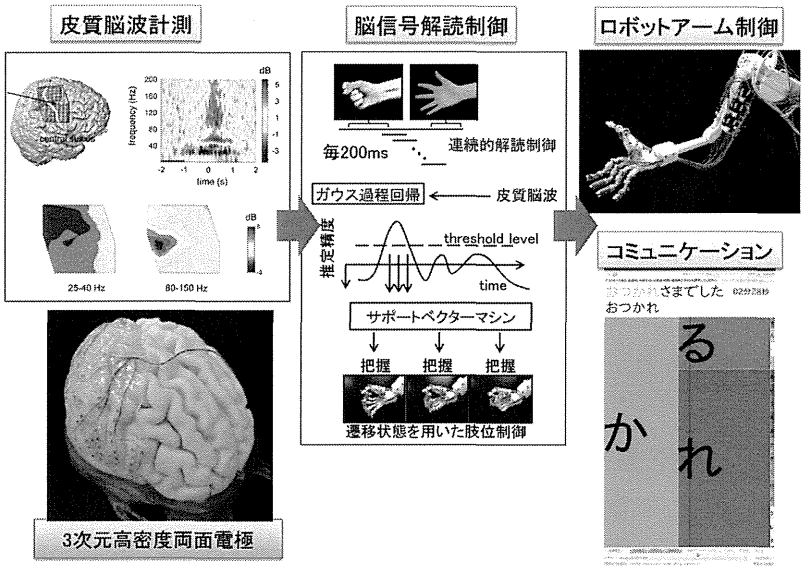

図3　皮質脳波BMIによる運動・意思伝達支援システム

2-2.ワイヤレス体内埋込装置

ワイヤレス体内埋込装置の研究開発に関しては、これまでに128ch装置のプロトタイプを開発し（図4）[12)、13)]、これをサルに埋込可能なサイズに小型化した装置を用いて急性期実験と長期埋込実験をおこなったところである。

本装置は頭部装置と腹部装置からなる。頭部装置は、3次元高密度両面電極、マルチチャンネル集積化アンプとアンプを収納する人工頭蓋骨兼用頭部ケーシングからなる。腹部装置は、ワイヤレスデータ通信回路、非接触充電電源とそれらを収納する腹部ケーシングからなる。

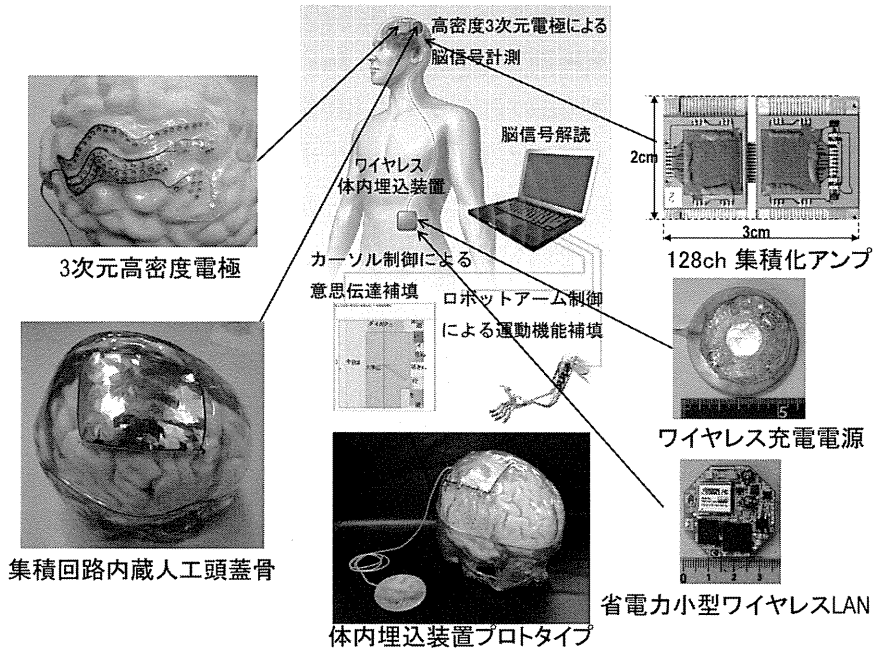

図4　BMI用ワイヤレス体内埋込装置

3次元高密度両面電極はテーラーメイドにより個々人の脳形状にフィットするものを考案した（図5）[14)、15)]。脳表面形状抽出は、Thin slice MRI画像を用いて行い、特に脳溝形状データについては自動脳溝抽出ソフト（Brain VISA、http://brainvisa.info/）を用いた形状抽出を行う。これらの脳形状データから3次元CAD（3 matic、Mimics、Materialize Japan、Tokyo）上で電極配置を最適化してシート型の設計を行い、3次元プリンタで型を

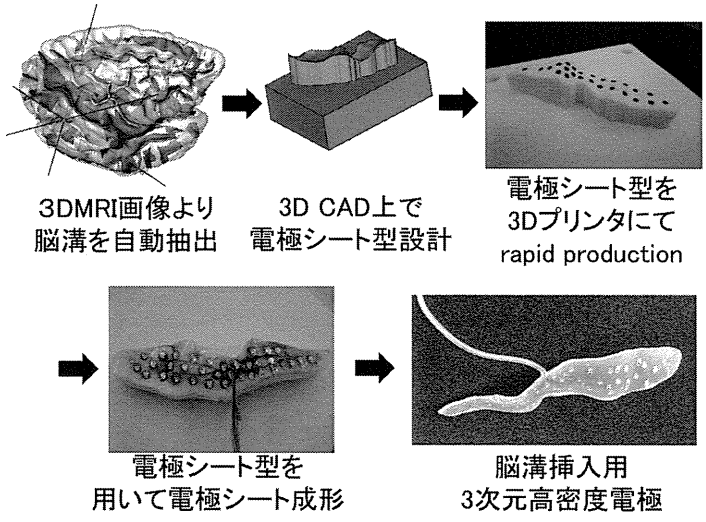

図5　3次元高密度電極の製造方法

迅速製造する。個々人の脳形状に密着するため、全ての電極から精度の高い皮質脳波が計測でき、脳への圧迫も少ない。電極間距離は最高2.5mmで従来の電極間隔10mmに比較して16倍高密度化した。電極は電極径1mmの白金電極を用いている。極端に小型化すると計測安定性が低下する懸念があるが、同一の電極を用いたサルの実験で1年間にわたり安定して計測できることが示されている[16]。脳溝内に挿入する場合には両面に電極を配置できる。

計測した皮質脳波はノイズ混入を防ぐため、すぐに増幅・デジタル化する必要がある。そこで頭部の狭小なスペースに留置できるよう皮質脳波を増幅するアナログアンプを集積化した。1チップあたり64chを有し、各chは1kHzでのサンプリングが可能であり、ADコンバーターは12bit、チップサイズは5×5mm、消費電力は4.9mWである[17]。東京大学VDECのCMOS 0.18umプロセスにて製造した。これを2チップ計128chとして30×20×2.5mm大の小型基板上に実装する。この集積化アンプ実装基板は人工骨兼用頭部ケーシングに収納される。

頭部ケーシングは、集積化アンプを収容し、開頭部の人工頭蓋骨を兼ねるものを考案した[18)、19)]。Thin slice bone window CT画像から3次元CAD（3 matic、Mimics、Materialize Japan、Tokyo）上で、開頭範囲、人工頭蓋骨の形状、電子回路のレイアウト設計を行い、3次元CAM（Gibbs CAM、Gibbs and Associates、USA）で切削パスを作成し、迅速製造する。患者CT画像から骨データを抽出して作成し、人工頭蓋骨を兼ねるため埋込による皮膚膨隆がなく、整容学的に優れ、瘻孔形成等のリスクも低い。開頭は頭部ケーシングに合わせて正確に開頭する必要があるため、頭部ケーシングの位置形状データをナビゲーションにあらかじめレジストレーションしておき、ナビゲーションガイド下に開頭を行う。

ワイヤレス通信モジュールはWifiプロトコールを採用し1.6Mbpsの速度で128ch、12bit、1kHzの皮質脳波データを伝送する[13]。平均消費電力80mWである。非接触充電は400mWの電力を皮下20mmの距離で充電可能である。

動物実験に関しては、急性期実験にて皮質脳波が計測できて、サルの上肢運動にともなって生じるhigh γ帯域活動を検出できること、末梢感覚神経電気刺激に対する大脳皮質の反応を検出できること等を確認できた。また6ヶ月間の長期埋込実験では耐久性、安全性に基本的な問題がないことを確認したところである。

今後の研究課題としては、これまでに開発した装置が動物実験レベルの装置であるのに対して、今後は体内埋込医療機器として薬事承認が得られる臨床レベルの仕様を満たした装置の開発が必要であると考えられる。

3．2023年の将来展望

3-1.皮質脳波BMIの用途・応用展開などの可能性

皮質脳波BMIはまず身体障害者の機能代替装置としての用途が考えられる。対象疾患と

しては、筋萎縮性側索硬化症、筋ジストロフィー等の神経難病、脊髄損傷、特に頚髄損傷、切断肢、脳卒中後遺症等が挙げられる。後述するようにBMI技術の進歩により、対象疾患は指数級数的に増大すると期待される。身体障害者は運動、意思伝達だけでなく嚥下機能にも障害を抱えている場合が多く、将来的には嚥下機能もBMIにより代替・支援することにより、より総合的に身体障害者のQOL向上に貢献できると考えられる。

皮質脳波BMIは手術を必要とするため身体障害者が主な対象となるが、高齢者についても将来的には対象となる可能性がある。認知症はないが、四肢の機能の衰えにより移動等が困難になっている要介護の高齢者が対象となろう。

ワイヤレス体内埋込装置の応用展開として、難治性てんかん患者のてんかん焦点同定を目的とした埋込型ないし携帯型脳波計への応用が考えられる。さらに電気刺激機能を付加するとてんかん発作を皮質脳波計測により検知して、電気刺激により発作を停止する埋込型てんかん発作制御装置として応用展開が可能となる。薬剤の効果がない難治性てんかんの治療に有効な手段となる可能性がある。

3-2.経済性や市場性展望

皮質脳波BMIの技術レベルの進歩して解読・制御が詳細になれば、適応疾患が拡大市場が拡大する（図6）。ALSは進行性の疾患で最終的に全身の筋肉が完全に麻痺するため最重症であり、現状ではALS患者に対する運動・意思伝達支援としての実用化が最も近いと考えられる。しかし患者は国内8000人、世界35万人にとどまり、市場規模は小さい。BMIによるロボットアーム操作の性能が向上して思い通りにロボットアームを制御できるようになれば、上肢の麻痺した頚髄損傷患者や半身麻痺の脳卒中後遺症患者に適用範囲が拡大すると考えられる。脊髄損傷は国内10万人、脳卒中後遺症患者は国内150万人と、患者数は

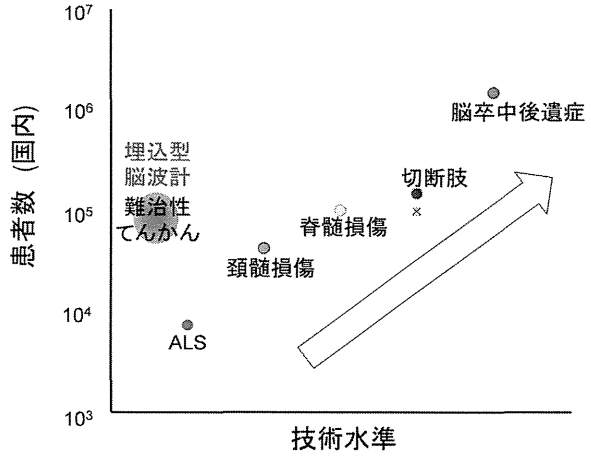

図6　BMIの技術水準と市場規模
BMIの技術水準が上がると市場規模は指数級数的に増える。

非常に多く、この段階では国内だけで市場規模は十分となる。

3-3.皮質脳波BMIの実現に向けて鍵を握るポイント・実現時期

皮質脳波BMIの実用化が実現するために最も重要なポイントは企業化ができるかどうかにかかっている。装置の製造・販売、メンテナンス、サポートサービスを行う企業がいなければ、この技術を継続的に提供・サポートすることはできない。体内埋込医療機器は薬事認可においてClass 4という最もハードルの高い分野であり、またトラブルが発生したときのイメージダウンが大きく、賠償責任も重いため、企業は参入を躊躇する場合が~~多いのが実情である。~~

本邦の薬事承認プロセスが遅いことは周知の事実であり、処理の迅速化が実現時期に大きく影響を与えると考えられる。本邦では国産の体内埋込装置の開発・実用化の経験がほとんどないため、薬事承認を行うこと自体にも大きな困難を伴うと考えられる。そこでこれらを少しでも軽減するため、我々は皮質脳波BMIの審査に関するガイドラインの策定を行った[20]。こうしたガイドラインも技術の進歩に合わせて今後、改訂を行うとともに、開発に関するガイドライン策定も要望されるところである。

装置開発には多額の開発費がかかるため、国の大型プロジェクトによる支援が必要である。また初期のALS患者に対するBMI装置の実用化段階では、依然BMI装置のコストが高いため、ALS患者がBMI装置を導入する際には国による導入資金援助が必要となろう。

3-4.10年後の到達点展望

10年後には、重症ALSや筋ジスの患者を対象として、128chワイヤレス体内埋込装置を用いた運動・意思伝達支援システムが実用化していると期待される。また、脳信号解読・制御技術の進歩により、ロボットアーム、コンピュータ制御が精緻化し、脊髄損傷、切断肢、脳卒中患者への適応拡大が検討されていると期待される。

装置開発では現在すでに~~開発が開始されている~~1000ch規模の次世代体内埋込装置の実用化開発が進んでいると考えられる。さらに、フレキシブル有機集積化技術[21]を用いた次々世代体内埋込装置の技術開発が進み、実用化開発へステップアップする時期になっていると予想される。

4．皮質脳波BMIに関する主な研究機関・企業・研究者

大阪大学脳神経外科：平田雅之、吉峰俊樹、柳澤琢史、松下光次郎

ATR脳情報総合研究所：川人光男、神谷之康

情報通信研究機構：鈴木隆文

電気通信大学：横井浩史